Electronic Structure and Spectra of Organic Dye Anions of Uranine and Eosin Y

Koichi HIRANO

Department of Chemistry, Miyagi University of Education, Aramaki-aoba, Sendai 980

(Received May 14, 1982)

The excited states of the organic dye anions of Uranine and Eosin Y are invesitigated by the semi-empirical SCF-MO-CI calculations. The two-center core integral values of the C–Br bond (−0.20 eV) were determined. Agreement between the calculated and observed spectra was satisfactory. The first intense bands of these dye anions can be assigned to the HOMO→LUMO transition band arising from the local excitation of xanthene ring. The second bands are interpreted as the overlap of the two transition bands for the xanthene ring and for the residual π-systems.

Because of the interest in the metachromatic changes exhibited by many dye ions,[1–5] we have made experimental studies on the solvato-chromic effects of several xanthene dyes.[6] We analyzed the solvent effects on the Eosin Y spectra using the modified McRae's theory,[7] and determined separately the values of the dispersion shift and the hydrogen bond shift.[8] In addition, an attempt was made to estimate the electrostatic shifts for Eosin Y anion by means of Hückel MO perturbation theory.[9] It was concluded that quantitative knowledge about the electronic transitions of the solute dye ions is needed to obtain a deeper understanding of the solvato-chromic effects. For xanthene dyes including Uranine and Eosin Y, however, very little is known about the nature of the electronic transitions.

The main aim of this invesitigation is to gain information about the electronic transitions of Uranine and Eosin Y anions. For this purpose, the lower excited states of the anions of Uranine ($URAN^{2-}$) and Eosin Y ($EOSY^{2-}$) were invesitigated using semi-empirical SCF-MO-CI calculations.

Theoretical

Methods and Models. The Pariser-Parr-pople type of SCF-MO calculations[10,11] with limited D–CI were employed. In these calculations, singly-excited configurations higher than the ground configuration by 10 eV, and doubly-excited configurations higher than the ground configuration by 18—25 eV, were taken into account. The equal charge sharing models (see Fig. 1), in which a formal negative charge is equally shared between the two oxygen atoms O (24) and O(25), were considered for each of the anions. The attached benzene ring with a carboxy group cannot rotate freely around the C(14)–C(15) linkage, because of its steric hindrance.[12] We determined the dihedral angle to be $\theta=73°$ from the sum of the van der Waals radi of C(3) and C(23).[13] The molecular geometry used were assumed as follows: All bond angles equal to 120° and C(14)–C(15)=1.51,[14] C(21)–C(22)=1.24, C(21)–C(23)=1.24,[15] C(5)–O(24)=1.26, C(10)–O(25)=1.26,[16] C(3)–Br(26)=1.89,[17,18] C(6)–O(7)=1.39, and aromatic C–C bond lengths equal to 1.39 Å.

Parametrization. One-center-core and repulsion integrals W's, γ_{rr}'s were evaluated from the valence state ionization potentials and electron affinities. Two-center-core integrals, β_{rs}'s were calculated by the

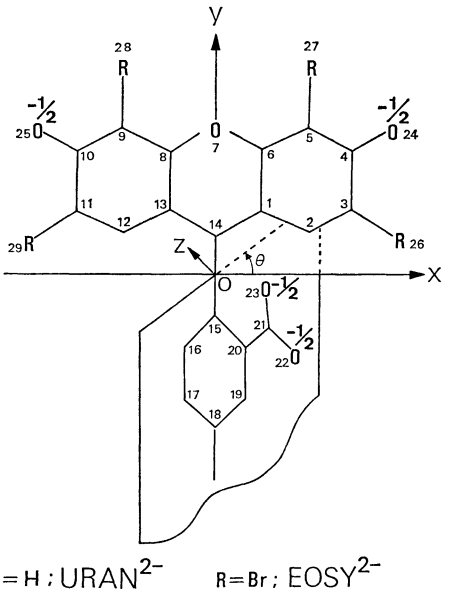

Fig. 1. Nuclear skelton and coordinate of an equal charge sharing model of $URAN^{2-}$ and $EOSY^{2-}$ anions. Dihedral angle θ is measured clockwise from the plane of the xanthene ring.

Wolfsberg-Helmholtz's formula.[19] Taking account of the rotation of the benzene ring, the two-center core integral for the C(14)–C(15) bond was formulated by Eq. 1;

$$\beta_{14,15} = \frac{K}{2} S_{14,15}(\theta=0°)\{W_{14}+W_{15}\}\cos\theta, \qquad (1)$$

where, θ is the dihedral angle, $S_{14,15}$ the overlap integral between C(14) and C(15), and K a constant taken to be 0.96 when β_{CC} in benzene is −2.39 eV. For the carbonyl and carboxy oxygen, $W_O^{-1/2}$ is taken as the arithmetic mean of W_O and $W_{O(-)}$; $W_{O(-)}$ is determined by a method identical with that previously reported by Nishimoto and Förster.[20] The two-center-repulsion integrals γ_{rs} were evaluated by the Nishimoto-Mataga's formula.[21] In the present calculations, the Br atom is assumed to participate in the pi-electronic system with a 4p lone electron-pair.

However, we have no available parameters for the atom, so we determined that parameter by following procedure. A one-center-core integral W_{Br} is estimated from the second ionization potential of the free Br atom.[22] The one-center-repulsion integral, γ_{BrBr}, and the effective nuclear charge, Z_{eff}, were evaluated by Morita-Dewer's formula.[23] The two-

Table 1. Parameters

Core	W_{rr}/eV[a]	$\langle rr\|rr\rangle$/eV[b]	Q_r[c]	Z_r^{eff}[d]	A_r/Å[e]
C^+	11.22	10.06	1.00	3.25	1.358
O^+	17.70	15.23	1.00	4.08	0.9453
O^{2+}	33.90	18.93	2.00	5.65	0.7606
$O^{-1/2}$	17.70	15.23	1.00	4.08	0.9453
$O^{(-)}$	17.70	15.23	1.00	4.08	0.9453
Br^{2+}	21.60	13.80	2.00	4.21	1.043

a) W_{rr}: Valence-state ionization potential. b) $\langle rr|rr\rangle$: One-center repulsion integral. c) Q_r: Core charges on atom r. d) Z_r^{eff}: Effective nuclear charge. e) A_r: $A_r=14.398/\langle rr|rr\rangle$ (Å).

center-core integral, β_{CBr}, was regarded as a parameter. Preliminary calculations were made by changing β_{CBr}, from -0.1 to -1.0 eV; an appropriate value of this parameter was determined as $\beta_{CBr}=-0.2$ eV. This value is lower than that estimated for 3-bromophenanthrenquinone molecule by Kuboyama *et al.*[24] A major source of this difference is that in negative ions, the pi-electrons are much more weakly bound and the spatial distribution of the electrons is more diffuse.[25,26]

Subsequently the correct β_{CBr} would be lower in magnitude than that estimated from a Slater type 4p orbital. The parameters finally employed were listed in Table 1.

Experimental

Uranine and Eosin Y obtained commercially were purified in the manner described previouly.[6] Wako Junyaku, Spectro grade, acetonitrile was used without further purification.

Visible and ultraviolet absorption spectra were measured on a Shimadzu UV200-S spectrophotometer. All the measurements were carried out at 25.0 °C.

Results and Discussion

Characteristics of Molecular Orbitals. The SCF-MO energy levels considered in CI calculation are illustrated in Fig. 2. One of interesting features found in the energy-level diagrams is that the HOMO of $URAN^{2-}$ is localized on C=O, whereas that of $EOSY^{2-}$ is localized both on C=O and Br. This indicates that in $EOSY^{2-}$ C=O and Br make dominant contributions to the lower energy excitations arising from the HOMO to the appropriate unoccupied MO's.

Another feature found in the energy diagram for $EOSY^{2-}$ is that the four new levels that originated from the 4p Br orbitals are closely located just below the HOMO level, so that the HOMO level is slightly destabilized. This orbital energy destabilization produces a red shift in the lowest energy absorption band of $EOSY^{2-}$ in comparison with that of $URAN^{2-}$.

Transition Energies and Oscillator Strengths. The calculated and experimental transition energies and oscillator strengths were shown in Table 2, where the calculations without D-CI are also shown for the sake of comparision. Agreement between the calculated and experimental values is satisfactory, excepting the oscillator strength for the lowest transitions of both

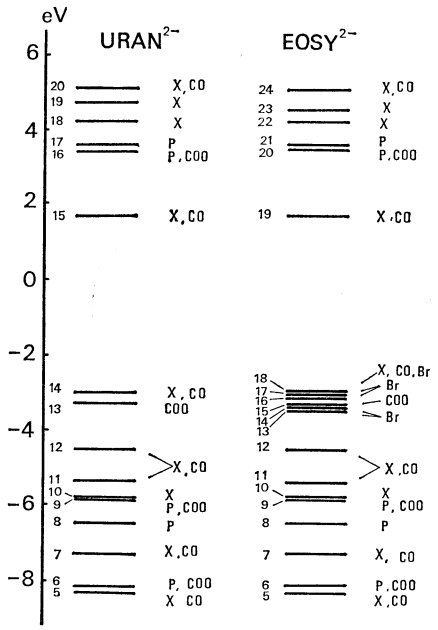

Fig. 2. MO energy-level diagrams for $URAN^{2-}$ and $EOSY^{2-}$, together with the orbital character. Symbol P and X designate the MO of phenyl and xanthene groups, respectively.

dye anions. As is shown in the table, the D-CI procedure does not always reduce the value of oscillator strengths, but it does enhance that value. This unexpected result may be partly ascribable to the fact that in our calculations, the number of doubly-excited configurations is not sufficiently large.

MO Coefficient Diagrams. The ground and excited state functions Ψ_J ($J=0$, $a,b,c,..$) are listed in Table 3. In the table, the configurations whose weight of mixing is larger than 2.0%, are given. On the basis of the main terms of the ground state functions, the MO coefficient diagrams associated with the excitations $\Psi_{i\to m}$'s$\leftarrow\Psi_G$ can be constructed from the one electron molecular orbitals of ϕ_i and ϕ_m as is shown in Figs. 3—4.

Electronic Spectra of $URAN^{2-}$. The calculated and observed spectrum of an acetonitrile solution of $URAN^{2-}$ are shown in Fig. 5. In the absorption spectrum of an acetonitrile solution of $URAN^{2-}$, we can see four π—π^* transition bands at 19.5, 32.5, 37.2, and 43.9×10^3 cm^{-1}. The additional tail at lower energy side ($22—23\times10^3$ cm^{-1}) may be ascribed to the singly ionized species.[27] The first high intensity visible band (1) is assigned to the transition $\Psi_a\leftarrow\Psi_0$, designated by line (a), which is mainly contributed by a HOMO→LUMO transition arising from the local excitation of xanthene ring (Fig. 3). The second weaker band (2), is regarded as the overlap of the two different types of transitions $\Psi_b\leftarrow\Psi_0$ and $\Psi_c\leftarrow\Psi_0$, denoted by (b) and (c): $\Psi_b\leftarrow\Psi_0$ Originates from the excitation of the attached benzene ring with carboxy group, whereas $\Psi_c\leftarrow\Psi_0$ originates from the excitation of the xanthene ring (Fig. 3). The third band (3) may be regarded as the superposition of the two transitions (d) and (e), although this assignment may not be unique. The predicted polarization direc-

Table 2. Transition energies ($\Delta E(10^3\,cm^{-1})$), oscillator strengths (f) and polarization($\phi°$)

URAN^{2-}

Transition	S-CI			D-CI			Obsd	
	ΔE	f a)	ϕ b)	ΔE	f a)	ϕ b)	ΔE	f
a	22.3	1.642	1.6	22.3	1.655	1.7	19.5	0.251
b	30.9	0.065	−72	31.1	0.065	−72		
c	33.0	0.172	−87	33.2	0.172	−87	32.5	0.081
d	36.1	0.361	−83	36.3	0.363	−83		
e	38.1	0.136	56	37.3	0.132	71	37.2	0.092
f	48.2	0.096	−31	48.4	0.097	31	43.9	0.670

EOSY^{2-}

Transition	S-CI			D-Cl			Obsd	
	ΔE	f a)	ϕ b)	ΔE	f a)	ϕ b)	ΔE	f
a	20.6	1.130	0.73	20.2	1.360	1.6	18.9 19.3 c)	0.427
b	20.9	0.300	3.2					
c	21.9	0.070	−0.14	22.0	0.069	−7.9		
d	23.1	0.079	−8.0	23.2	0.082	−6.1		
e	30.9	0.064	−72	31.3	0.065	−72	31.2	0.144
f	32.8	0.132	−88	32.9	0.118	−88		
g	34.2	0.113	−90	33.9	0.132	−85		
h	36.2	0.165	90	36.3	0.146	85	38.2	0.294
i				44.1	0.141	86	41.2	0.765

a) Oscillator strength greater than 0.05. b) The polarization vector is projected along the z-axis and angle ϕ was taken in a right-handed sense against the x-axis. c) For gaseous EOSY^{2-} determined from the spectral solvent effects.[3]

Table 3. Ground and excited wave functions of URAN^{2-} and EOSY^{2-}

URAN^{2-}	EOSY^{2-}
$\Psi_0=0.999\Psi_G$ a) $+\cdots$	$\Psi_0=0.999\Psi_G+\cdots$
$\Psi_a=0.985\Psi_{14\to15}+\cdots$	$\Psi_a=0.951\Psi_{18\to19}+0.206\Psi_{17\to19}+\cdots$
$\Psi_b=0.988\Psi_{13\to16}+\cdots$	$\Psi_c=0.981\Psi_{14\to19}+0.137\Psi_{16\to19}+\cdots$
$\Psi_c=0.880\Psi_{12\to15}-0.272\Psi_{14\to18}+\cdots$	$\Psi_d=0.991\Psi_{13\to19}+\cdots$
$\Psi_d=0.837\Psi_{14\to18}+0.345\Psi_{11\to15}-0.275\Psi_{10\to15}+\cdots$	$\Psi_e=0.989\Psi_{15\to20}+\cdots$
$\Psi_e=-0.661\Psi_{14\to19}+0.646\Psi_{10\to15}-0.255\Psi_{14\to18}+\cdots$	$\Psi_f=0.829\Psi_{12\to19}-0.320\Psi_{18\to24}+\cdots$
$\Psi_f=0.901\Psi_{12\to18}+0.362\Psi_{14\to19}+\cdots$	$\Psi_g=0.783\Psi_{11\to19}-0.453\Psi_{12\to19}-0.342\Psi_{18\to22}+\cdots$
$\Psi_g=0.862\Psi_{9\to16}-0.395\Psi_{8\to17}-\cdots$	$\Psi_h=-0.568\Psi_{18\to23}-0.510\Psi_{18\to22}+0.280\Psi_{14\to22}-0.255\Psi_{16\to22}+\cdots$
	$\Psi_i=0.853\Psi_{9\to19}-0.254\Psi_{17\to22}+\cdots$
	$\Psi_j=0.585\Psi_{17\to22}-0.499\Psi_{16\to23}+0.351\Psi_{13\to21}+\cdots$

a) G: Ground configuration.

tion of transition (*a*) is along the x-axis and those of (*b*) and (*c*) are along the y-axis. This agree well with the prediction based on the fluorescence polarization measurements.[28]

Electronic Spectra of EOSY^{2-}. The absorption spectra of acetonitrile solution of EOSY^{2-} and URAN^{2-} generally resemble (Figs. 5, 6): There are four π—π^* transition bands at 18.9, 31.2, 38.2, and 41.2×10^3 cm^{-1} (Fig. 6). The first intense band (1) shows a small red shift in comparision with the corresponding band of URAN^{2-}. This is interpreted in terms of orbital destabilization due to the substituent effect with bromine. This band is assigned to the transition $\Psi_a\leftarrow\Psi_0$ mainly contributed by a HOMO→LUMO transition, arizing from the local excitation of the xanthene ring. A chracteristic feature of this transition is that on going from Ψ_0 to Ψ_a, a substantial amount of charge transfer from the carbonyl oxygen ($-0.127e$) and from the bromine substituents ($-0.229e$) into the xanthene ring, especially the central carbon atom C(14), the latter being primary (Fig. 4). The second weaker band (2) is regarded as the overlap of the transitions $\Psi_e\leftarrow\Psi_0$ and $\Psi_f\leftarrow\Psi_0$ denoted by (*e*) and (*f*). Transition $\Psi_e\leftarrow\Psi_0$ has almost the same nature as that of $\Psi_b\leftarrow\Psi_0$ for URAN^{2-} which has been already been described. Transition $\Psi_f\leftarrow\Psi_0$, however, is somewhat different in nature from that of $\Psi_c\leftarrow\Psi_0$ for URAN^{2-}: On going from Ψ_0 to Ψ_f, the charge tend to move away from the xanthene ring to the carbonyl oxygen (Fig. 4). The third band (3) may be assigned to the superposition of the transitions (*g*) and (*h*), however, the fourth band (4) cannot be assigned to the calculated transitions.

Neither the transition energies nor the oscillator

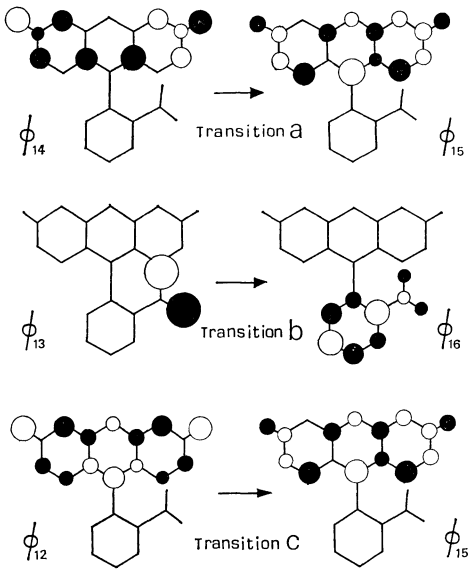

Fig. 3. Schematic representation of MO coefficients for URAN^{2-} associated with three lowest excitations.

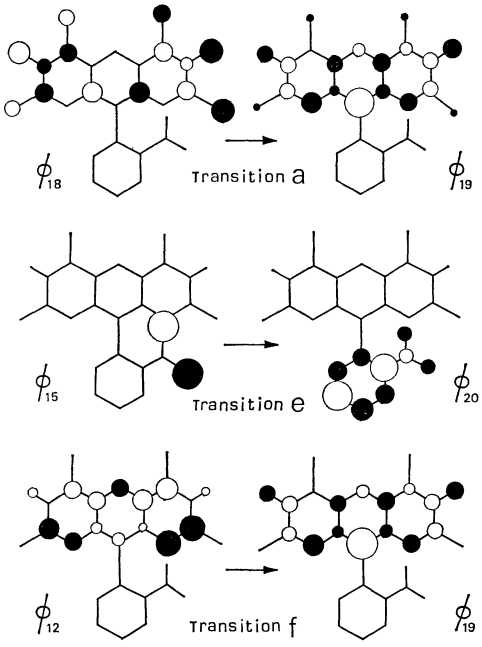

Fig. 4. Schematic representation of MO coefficients for EOSY^{2-} associated with three lowest excitations.

strengths were affected by changes of the dihedral angle θ. This is consistent with the transitional characteristics of these dye anions.

We wish to express our hearty thanks to the members of the Computer Center Tohoku University for their kind cooperations and advice. This work supported in part by a scientific Research Grant from the Ministry of Education, Science and Culture, Japan (No. 538029).

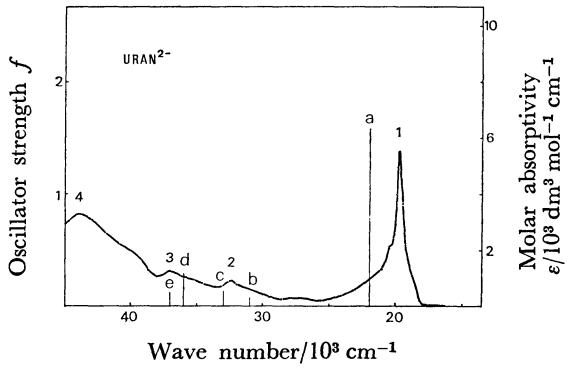

Fig. 5. Absorption spectrum of URAN^{2-} in acetonitrile solution at 25.0 °C; 1.14×10^{-5} mol dm^{-3}.
The vertical lines represent the calculated transition energies and oscillator strengths greater than 0.05.

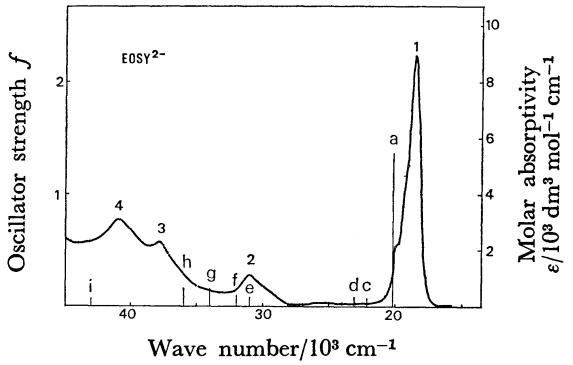

Fig. 6. Absorption spectrum of EOSY^{2-} in acetonitrile solution at 25 °C; 1.49×10^{-5} mol dm^{-3}.
The vertical lines represent the calculated transition energies and oscillator strengths greater than 0.05.

References

1) P. Ehrlich, *Arch. Mikroskop. Anat. Entwick.*, **1877**, 13.
2) L. Michaelis and S. Granick, *J. Am. Chem. Soc.*, **67**, 1212 (1945).
3) H. Terayama, *Kagaku No Ryoiki*, **1**, 17 (1947).
4) M. Koizumi and N. Mataga, *J. Am. Chem. Soc.*, **75**, 483 (1953).
5) K. Hirano, *Biophysics (Seibutu-Buturi)*, **19**, 38 (1979).
6) K. Hirano, *Nippon Kagaku Kaishi*, **1974**, 1823.
7) K. Hirano, *Nippon Kagaku Kaishi*, **1978**, 481.
8) K. Hirano, *Nippon Kagaku Kaishi*, **1980**, 675.
9) K. Hirano, *Nippon Kagaku Kaishi*, **1976**, 361.
10) R. Pariser and R. G. Parr, *J. Chem. Phys.*, **21**, 446 (1953).
11) J. A. Pople, *Trans. Faraday Soc.*, **49**, 1375 (1953).
12) S. E. Sheppard, *Rev. Mod. Phys.*, **14**, 317 (1942).
13) J. Silverman and N. F. Yannori, *J. Chem. Soc., B*, **1967**, 194.
14) H. Suzuki, *Bull. Chem. Soc. Jpn.*, **32**, 1340 (1959).
15) J. M. Skinner, G. M. D. Stewart, and J. C. Speakman, *J. Chem. Soc.*, **1954**, 180.
16) The bond length of C=O's were estimated from the SCF pi-bond order, according to C. A. Coulson, *Proc. R. Soc. London, Ser. A*, **169**, 413 (1939).
17) T. Sato. M. Shiro, and H. Koyama, *J. Chem. Soc., B*, **1962**, 935.
18) M. Tabata, Y. Takada, and A. Suzuki, *Chem. Lett.*, **1972**, 1092.

19) M. Wolfsberg and L. Helmholtz, *J. Chem., Phys.*, **20**, 837 (1952).
20) K. Nishimoto and L. Förster, *J. Phys. Chem.*, **72**, 914 (1968).
21) N. Mataga and K. Nishimoto, *Z. Phsik. Chem. Neue Folge*, **13**, 140 (1957).
22) C. E. Moor, "Atomic Energy Levels," National Burau of Standers, Washington (1949), Circ. No. 467, Vol. I—III.
23) M. J. S. Dewer and T. Morita, *J. Am. Chem. Soc.*, **91**, 796 (1969).
24) A. Kuboyama, F. Kobayashi, and S. Morokuma, *Bull. Chem. Soc. Jpn.*, **48**, 1245 (1975).
25) H. Tsubomura and S. Sunakawa, *Bull. Chem. Soc. Jpn.*, **40**, 2463 (1967).
26) A. H. Zimmerman, R. Gygax, and J. I. Brauman, *J. Am. Chem. Soc.*, **78**, 5595 (1978).
27) F. M. Abdel-Halim, R. M. ISSA, M. S. El-Ezaby, and A. A. Hasein, *Z. Phys. Chem. Neue Folge*, **73**, 50 (1970).
28) A. Wrazeesinska, *Acta Physik. Polan.*, **4**, 486 (1935).